Conduction-band states of TiS_2 studied by means of polarized x-ray absorption

F. Antonangeli and M. Piacentini
Istituto di Struttura della Materia del Consiglio Nazionale delle Ricerche, Via Enrico Fermi 38, I-00044 Frascati, Italy

R. Girlanda* and G. Martino*
Istituto di Struttura della Materia, Università degli Studi di Messina, I-98100 Messina, Italy

E. S. Giuliano*
Istituto di Fisica Teorica, Università degli Studi di Messina, I-98100 Messina, Italy
(Received 24 May 1985)

We studied the polarization dependence of the Ti K threshold in the layered compound TiS_2. We found that the weak structures at about 4967 eV associated with the Ti empty d states are dipole allowed for $\mathbf{E}\perp\mathbf{c}$, and that the following sharp, strong peak at 4975.7 eV is isotropic. With the multiple-scattering method, we calculated the projected densities of states that reproduce our polarization-dependent spectra, except for the d structures and the sharp peak at 4975.7 eV. The former can be interpreted with consideration of the TiS_2 band structure. For the latter we suggest a bound state or resonance of the excited crystal.

I. INTRODUCTION

TiS_2 is a layered material that has attracted considerable attention in recent years, especially for its important role as cathode material in batteries based on Li^+ transport. In fact, Li^+ ions can be intercalated into the van der Waals gaps between the (S-Ti-S) slabs, but there is no real understanding of the bonding mechanism between the intercalate and the chalcogenide layer. Inside the single layer, the Ti atoms are octahedrally coordinated with six S atoms. Using the simple language of molecular orbitals, the Ti d states are split by the octahedral field into the t_{2g}-e_g levels.[1] Clearly, these levels in the crystal form two narrow bands. Higher empty states derive from the Ti $4s$ and $4p$ levels, with some admixture with the S $3p$ orbitals.[1] It is important to obtain as much information as possible on the lowest empty states, which are most likely involved in the intercalation process. In this respect, several core-level absorption measurements appeared,[1–4] but their interpretation is not yet satisfactory. We have investigated in detail the Ti K absorption edge with the purpose of clarifying some of the questions still open.

The Ti K threshold in TiS_2, likewise $TiSe_2$,[3] is formed by two weak features at 4966.8 and 4968.5 eV (see Fig. 1) that have been assigned previously to the Ti empty final d states.[3] Their separation of 1.7 eV is slightly smaller than the t_{2g}-e_g splitting of 2.0–2.3 eV determined with other techniques[1–5] or calculated theoretically.[6–10] These two d structures are followed by a strong, sharp, asymmetric peak at 4975.7 eV, attributed to final Ti p-like states.[3]

The two d structures are fairly strong, approximately 14% of the main peak, and their strength is not yet clear. In the cluster model the Ti $1s$-$3d$ transitions are dipole forbidden, but allowed in the quadrupole approximation. This selection rule is so strict that in bis-(creatinium)-tetrachlorocuprate(II), a complex containing $CuCl_4$ square planar units, the Cu $1s$-$3d$ peak is only 4% of the following dipole-allowed structure, and it has been demonstrated that it is a quadrupole-allowed transition by means of polarization-dependent experiments performed on oriented single crystals.[11] Fisher,[1] and subsequently Davies and Brown,[3] suggested that the hybridization of the Ti d orbitals with the ligand p states may be responsible for the observed intensity. However, the Ti $1s$—S $3p$ transition matrix element should be much smaller then the Ti $1s$-$4p$ transition matrix element, since it is a two-center integral. In addition, only even-parity combinations of the S $3p$ states can hybridize with the Ti $3d$ states. It is difficult to think that odd-parity combinations are degenerate in energy with the t_{2g}-e_g d-like levels, and once more the Ti $1s$-$3d$ transitions are dipole forbidden in the molecular approach.

In order to shed light on the type of transitions involved and on the nature of the empty states of TiS_2, we

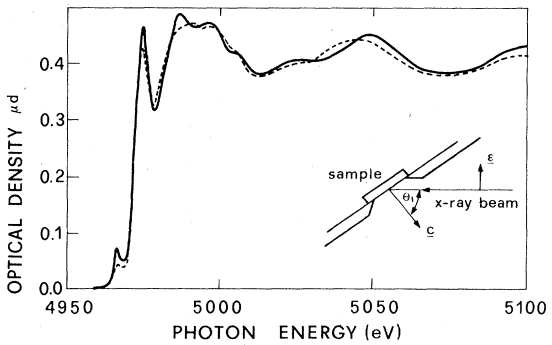

FIG. 1. Spectra of the optical density of the Ti K absorption in TiS_2. Solid line: $\theta_i=0°$. Dashed line: $\theta_i=55°$. The $\theta_i=55°$ spectrum has been corrected for the longer path of the radiation inside the sample at oblique incidence. The inset shows schematically the experimental setup.

measured the dichroism of the x-ray absorption at the Ti K threshold. We found that the d structures are dipole allowed for $\mathbf{E}\perp\mathbf{c}$ ($\mathbf{E}$ is the polarization versor of the x rays) and dipole forbidden for $\mathbf{E}\|\mathbf{c}$, and that the strong peak at 4975.7 eV is practically isotropic, as will be discussed in Sec. II. We have also calculated the projected density of states using the multiple-scattering method, described in Sec. III. The calculated projected densities of states agree well with several previous absorption[1–4] as well as emission[1,12] spectra, as shown in Sec. IV, and also explain the major features of our polarization-dependent spectra, except for the weak d structures and the sharp peak at 4975.7 eV. The former can be accounted for by considering the full crystalline band structure. For the latter we suggest that it derives from a resonance of the excited crystal.

II. EXPERIMENTAL

The measurements have been performed using the x-ray beam line of the Programma per l'Utilizzazione della Luce di Sincrotrone (PULS) facility at the Istituto Nazionale di Fisica Nucleare (INFN) National Laboratories in Frascati.[13] The synchrotron radiation collected from one of the Adone bending magnets was monochromatized with a channel-cut Si(220) crystal. The entrance and exit slits of the monochromator were set for the best compromise between high resolution and high photon flux. The overall band pass and the degree of polarization at the sample in the 5-keV region were 0.5 eV and 98%, respectively.

Small platelets of TiS_2, approximately 2×2 mm^2 large and a few μm thick, were obtained by peeling larger samples with adhesive tape. The platelets were mounted on a vertical shaft after proper masking, with horizontal $\mathbf{c}$ axis. By rotating the shaft, the angle of incidence θ_i of the radiation falling on the sample with p polarization could be varied, as sketched in the inset of Fig. 1.[14] The reading of the angles with respect to the normal incidence position was accurate within $\pm0.5°$. However, the normal incidence position was set by eye at the beginning of each group of measurements and a systematic error of a few degrees was possible. The leakage of x radiation through pinholes or the sides of the sample holder showed up as a saturation of the strongest structures in a few spectra measured at large angles of incidence.

A polynomial was fit to the pre-edge background and subtracted from all the measured spectra in order to obtain only the Ti K absorption spectra. The smooth, atomiclike absorption far above threshold should be isotropic and the optical density should scale with the angle of incidence according to

$$\mu d(\theta_i)=\frac{\mu d(\theta_i=0°)}{\cos\theta_i} \tag{1}$$

due to the increased path of the radiation inside the samples (see the inset of Fig. 1). If the normal incidence position is set incorrectly, the isotropic absorption does not scale as from Eq. (1). Conversely, if $\cos\theta_i$ in Eq. (1) is used as a normalization constant, the value of θ_i so determined differs from the nominal value, the error increasing with the angle of incidence.

In Fig. 1 we show the Ti K absorption spectra extending well beyond threshold for $\theta_i=0°$ and 55°, respectively. The normal incidence spectrum is in perfect agreement with that reported by Davies and Brown.[3] The onset of the K absorption occurs at 4964.5 ± 0.5 eV, in agreement with the value reported by Bearden and Burr[15] for Ti metal and by Davies and Brown for $TiSe_2$,[3] and with the edge for K emission reported by Šimůnek *et al.* for TiS_2.[12]

The shape and general intensity of the spectrum at 55°, scaled according to Eq. (1), agrees with the normal incidence spectrum very well. However, remarkable anisotropies due to solid-state effects can be observed in the weak oscillations superimposed to the atomiclike absorption. The small variation of the intensity of the sharp peak at 4975.7 eV may be due to minor experimental errors, and we consider this peak to be practically isotropic. A strong dichroism characterizes the threshold itself, which is shown in detail in Fig. 2, where we present the absorption spectra, normalized to the peak at 4975.7 eV, measured near the threshold at several angles of incidence. The two weak d structures, generating a well-resolved peak at 4966.8 eV and a plateau around 4969 eV, tend to disappear in the spectra taken at the highest angles of incidence, leaving a smooth steplike, isotropic feature. Also, the shoulder observed in the $\theta_i=0°$ spectrum at about 4972 eV on the low-energy side of the 4975.7-eV peak is missing in the $\theta_i=75°$ spectrum.

We have fitted the intensity of the weak peak at 4966.8 eV with the relation

$$I(\theta_i)=A+B\cos^2\theta_i \tag{2}$$

as shown in the inset of Fig. 2. The $\cos^2\theta_i$ dependence

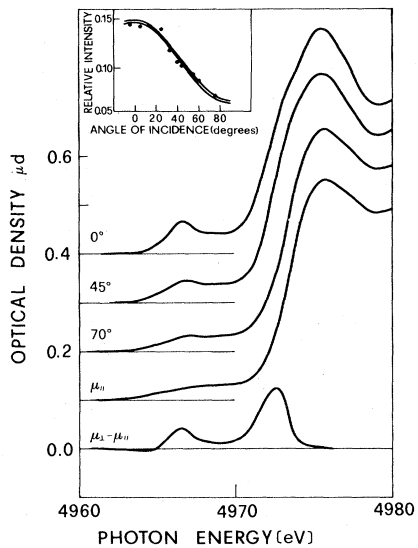

FIG. 2. Spectra of the optical density of the Ti K absorption threshold in TiS_2. The spectra have been displaced upwards with respect to each other for a better display. Also shown are the spectra of $\mu_{\|}$ and the difference $\mu_\perp-\mu_{\|}$ derived from the above spectra. The inset shows the best-fit curve of the intensity of the pre-edge structure at 4966.8 eV with Eq. (2).

corresponds to a transition that is dipole allowed for $\mathbf{E}\perp\mathbf{c}$ and dipole forbidden for $\mathbf{E}\|\mathbf{c}$. $B=0.076$ gives the intensity of the anisotropic peak, while $A=0.062$ gives the intensity of the isotropic background. From the spectra measured at several angles of incidence we calculated the spectrum for $\theta_i=90°$, shown in Fig. 2, from the relation

$$\mu(\theta_i)=\mu_\perp\cos^2\theta_i+\mu_\|\sin^2\theta_i\ , \tag{3}$$

where $\mu_\|$ and $\mu_\perp$ correspond to the absorption coefficient for $\mathbf{E}\|\mathbf{c}$ ($\theta_i=90°$) and $\mathbf{E}\perp\mathbf{c}$ ($\theta_i=0°$), respectively. Finally, we have calculated the difference spectrum $\mu_\perp-\mu_\|$, also shown in Fig. 2, in order to enhance the features allowed only for $\mathbf{E}\perp\mathbf{c}$ at 4966.8, 4968.5, and 4972.5 eV.

III. THEORY

The electronic properties of the transition-metal dichalcogenides have been extensively studied by many authors in terms of the band-structure theory (for details, see Ref. 16). However, the x-ray absorption, being a local process, is described better by means of the electronic density of states projected on the particular atom where the process occurs.

We have calculated the projected densities of states (DOS's) within the multiple-scattering approach applied to a finite cluster of atoms, the positions of which are chosen according to the corresponding crystal structure. The underlying idea is that such a finite system is able to describe the main features of the infinite system as far as local effects are concerned.

We build a cluster of nonoverlapping muffin-tin potentials centered at the atomic positions and we describe their scattering properties in terms of the corresponding phase shifts:

$$\delta_l(E)=\tan^{-1}\left[\frac{\sqrt{E}\,n_l'(\sqrt{E}\,|r|)-\gamma_l n_l(\sqrt{E}\,|r|)}{\sqrt{E}\,j_l'(\sqrt{E}\,|r|)-\gamma_l j_l(\sqrt{E}\,|r|)}\right]_{r=\mathbf{R}_{\mathrm{MT}}}, \tag{4}$$

where n_l and j_l are the spherical Neumann and Bessel functions, respectively, and $\gamma_l\equiv(1/R_l)(dR_l/dr)\,|_{r=\mathbf{R}_{\mathrm{MT}}}$. R_l are the solutions of the radial Schrödinger's equation:

$$\left[-\frac{1}{r}\frac{d^2}{dr^2}-\frac{l(l+1)}{r^2}+V_{\mathrm{MT}}(r)\right]R_l(r,E)=ER_l(r,E)\ . \tag{5}$$

From knowledge of the phase shifts we easily obtain the on-the-energy-shell matrix element of the transition matrix $t(E)$ as[17]

$$t_l(E)=-\frac{1}{\sqrt{E}}\sin\delta_l(E)e^{i\delta_l(E)} \tag{6}$$

which describes the scattering properties of that potential. Moreover, within the single-site approximation, the scattering properties of the whole system can be obtained from[18]

$$J^{ij}_{LL'}(E)=t^i_l(E)\delta_{ll'}\delta_{ij}+\sum_{k(\neq i)}\sum_{L''}t^i_l(E)G^0_{LL''}(\sqrt{E}\,|\mathbf{R}_i-\mathbf{R}_k|)J^{kj}_{L''L}(E)\ , \tag{7}$$

in which $L\equiv l,m$ and

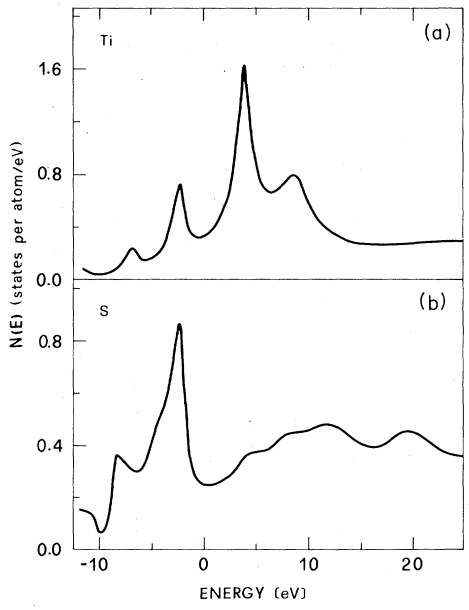

FIG. 3. Calculated densities of states for TiS_2 projected on (a) the Ti site and (b) the S site. The zero of the energy scale has been placed at the Fermi energy.

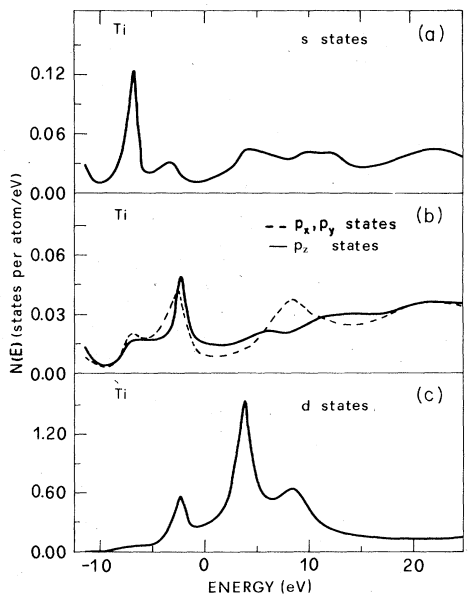

FIG. 4. Calculated densities of states for TiS_2 projected on the Ti site and separated into the angular momentum components.

$$G^0_{LL'}(\sqrt{E}\,|\,\mathbf{R}_i-\mathbf{R}_k\,|)=4\pi\sqrt{E}\sum_{L''} i^{l''}C^{L''}_{LL'}[n_{l''}(\sqrt{E}\,|\,\mathbf{R}_i-\mathbf{R}_k\,|)+ij_{l''}(\sqrt{E}\,|\,\mathbf{R}_i-\mathbf{R}_k\,|)]Y_{L''}(\Omega)\,, \tag{8}$$

where $C^{L''}_{LL'}$ are the Gaunt numbers,[19] and Ω is the angle between the directions $\mathbf{R}_i$ and $\mathbf{R}_k$.

As far as our purposes are concerned it has already been shown that the electronic density of states projected on a particular site i is given by[18]

$$N^i(E)=-\frac{E}{\pi}\sum_L\int_0^{R_{\rm WS}} dr\,r^2\,|\,R^i_l(r,E)\,|^2\frac{\mathrm{Im}J^{ii}_{LL}}{\sin^2\delta_l(E)}\,, \tag{9}$$

where the integral is extended to the Wigner-Seitz radius.

In Fig. 3 we present the density of states projected on the Ti atom [Fig. 3(a)] and on the sulfur atom [Fig. 3(b)]. We notice that the Fermi level lies in a region of minimum in the DOS's and that it is not possible to recover the small gap semiconductivity character of TiS_2 because of the finite number of atoms involved in our method. In Fig. 4 we present the DOS's projected on the Ti atoms separated in their angular momentum components and in Fig. 5 those projected on the S atoms.

We have checked our calculations by comparing them with other theoretical calculations as well as experimental results. A comparison of the total density of states of the valence bands with those calculated from the band structure of TiS_2 gives a good agreement. In addition, we find that the Ti p states contribute to the valence band for 0.4—0.5 electrons, which has to be compared with the results of Zunger and Freeman,[7] who obtained a promotion of 0.4 electrons from the Ti $4s$ states to the Ti $4p$ states using a different approach. In Fig. 6 we compare our projected DOS's with experimental soft x-ray absorption[1,2,4] and emission[1,12] spectra measured at several core thresholds of both the Ti and S atoms. The theoretical DOS's have been convoluted with Gaussian functions of half-width $\sigma=1.0$ eV. The agreement is very good for almost all the spectra, except for small energy shifts of the structures, possibly due to experimental uncertainties.

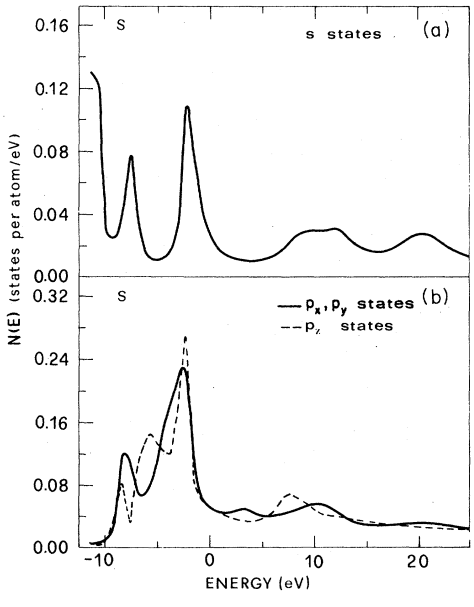

FIG. 5. Calculated densities of states for TiS_2 projected on the S site and separated into the angular momentum components.

IV. DISCUSSION

In the case of a $1s$ initial state, in a uniaxial system with the c axis in the z direction, the dipole selection rules allow final states with p_z symmetry for $\mathbf{E}||\mathbf{c}$ and p_x,p_y symmetry for $\mathbf{E}\perp\mathbf{c}$. Thus, in order to take into account these polarization effects, in Fig. 7 we compare the experi-

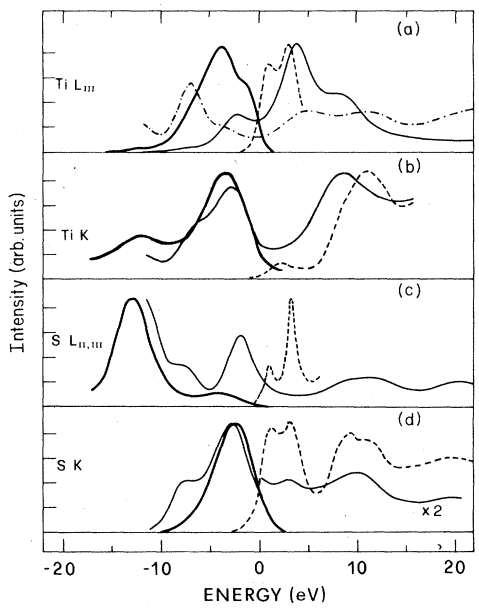

FIG. 6. Comparison between absorption and emission spectra measured for TiS_2 at several core levels of both Ti and S with the calculated projected densities of states. (a) Ti L_{III} edge. Heavy solid line: emission spectrum (Ref. 1). Dashed line: absorption spectrum (Ref. 1). Thin solid line: Ti projected d density of states. Dot-dashed line: Ti projected s density of states. (b) Ti K edge. Heavy solid line: emission spectrum (Ref. 12). Dashed line: absorption spectrum (present work, $\theta_i=0°$). Thin solid line: Ti projected p_x,p_y density of states. (c) S $L_{II,III}$ edge. Heavy solid line: emission spectrum (Ref. 1). Dashed line: absorption spectrum (Ref. 2). Thin solid line: S projected s density of states. (d) S K edge. Heavy solid line: emission spectrum (Ref. 1). Dashed line: absorption spectrum (Ref. 4). Thin solid line: S projected p_x,p_y density of states.

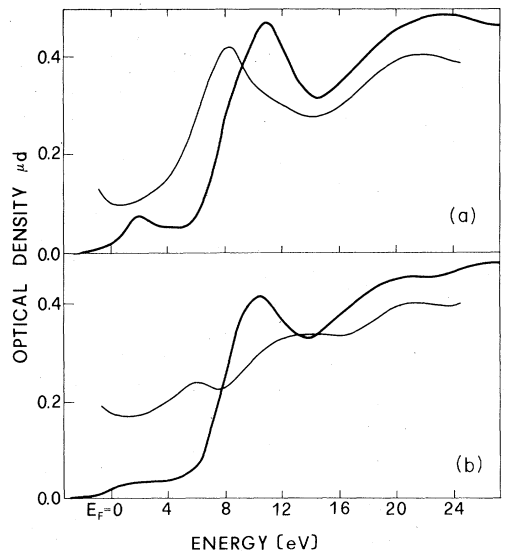

FIG. 7. (a) Experimental E⊥c Ti K absorption spectrum (heavy line) compared with the calculated Ti projected p_x,p_y density of states (thin line). (b) Experimental E||c Ti K absorption spectrum (heavy line) compared with the calculated Ti projected p_z density of states (thin line).

mental Ti K absorption spectra with the theoretical p_z and p_x,p_y DOS's projected on the Ti atom. The energy scale in Fig. 7 has been taken by aligning the theoretical Fermi level to the experimental threshold at 4964.5 eV.

The p_x,p_y DOS shows two main peaks at 8.4 and 21.5 eV, respectively, which could be associated with the experimental structures centered at 10.5 and 23.0 eV. If only the normal incidence spectrum were available, the agreement between theory and experiment should appear remarkably good, apart from the slight discrepancy in the energy positions of both peaks. However, the polarization-dependent measurements clearly indicate that such an assignment is incorrect. In fact, the first experimental peak at 10.5 eV is essentially isotropic, while the calculated peak at 8.4 eV in the p_x,p_y DOS is strongly anisotropic, since it is missing in the p_z DOS. For this reason, we do not associate the calculated structure at 8.4 eV to the strong, sharp peak at 10.5 eV, but rather to the shoulder at 8.2 eV, which is present only in the $\mu_\perp$ spectrum. On the other hand, the theoretical peak appearing in both p_x,p_y and p_z DOS's at $\sim$22 eV does not show anisotropic effects and it can be associated with the experimental structure at 23 eV. Finally, the trough at about 14 eV is less deep in the $\mu_{||}$ spectrum than in the $\mu_\perp$ one, in agreement with the presence of the broad feature in this region in the p_z DOS.

The weak pre-edge structure at 2.2 eV in the experimental spectrum is not reproduced by the p DOS's shown in Fig. 7. However, the d DOS shows a strong peak at this energy, supporting previous assignments to d-like final states.[3] The intensity of the experimental peak is approximately 4×10^{-3} times the intensity of the calculated one (the experimental d structure is about 15% smaller than the following p-like structures, and the calculated p-like peak at 22 eV is about 2.5% the d-DOS peak). This is an indication that transition matrix elements strongly reduce the transition probability. As a matter of fact, the Ti atom is at the center of a cluster with inversion symmetry, and so the Ti $1s$-d transitions are forbidden in the dipole approximation. This is valid even if hybridization of the Ti d states with S p states is present. Experimentally, we find that the 2.2-eV structure shows the polarization dependence characteristic for transitions that are dipole allowed only for E⊥c. Thus, for explaining its origin, we have to make use of the TiS_2 band structure. In fact, our scheme, as well as all calculations involving a finite number of atoms in real space, use a point group that corresponds to the point group at $\mathbf{k}=0$ in the Brillouin zone, where Ti p and d states cannot mix. Instead, near the Brillouin-zone boundaries, in particular at the K and H points, such a mixing is possible and the transitions from the Ti $1s$ states to the d-like ones become allowed only for E⊥c. It is worth noticing that the case of TiS_2 is different from that of bis-(creatinium)-tetrachlorocuprate(II), where the Cu ions do not interact with each other and its absorption spectrum is determined by the molecular selection rules. Thus, the Cu $1s$-$3d$ transitions are allowed only in the quadrupole approximation.[11]

TABLE I. Energies (in eV) of the experimental and calculated structures. The experimental energies are referred to the absorption threshold at 4964.5 eV.

Ti density-of-states features		Experimental structures E||c	E⊥c	
		27		Peak
p_x,p_y	22		23	Peak
p_z	20.5	20		Shoulder
p_z	13.6			
		10.5	10.5	Strong peak
p_x,p_y	8.4		8.2	Shoulder
p_z	6.0	4.5		Shoulder
d	3.5		2.2	Peak

In conclusion, the polarization dependence of the experimental absorption spectra can be reproduced well by our calculations, as summarized in Table I, with the exclusion of the strong, sharp structure at 10.5 eV. The threshold spectra in several other layered compounds, such as the Ga K edge in GaS and GaSe, show a shape and a behavior similar to the ones found here: a strong, almost isotropic peak, with a strongly anisotropic low-energy shoulder.[14] We believe that this behavior has a common origin for all these materials. We have shown that the shoulder can be interpreted as due to a peak present in the metal p_x,p_y projected DOS. In our opinion the strong isotropic peak that does not have its counterpart in the DOS's may be due to transitions at some bound or resonant state associated with the higher-energy isotropic p-like DOS peaks.

ACKNOWLEDGMENTS

We acknowledge the help and the support from the Programma per l'Utilizzazione della Luce di Sincrotrone (PULS) staff. This work has been partially supported by the Ministero della Pubblica Istruzione through the Gruppo Nazionale di Struttura della Materia (GNSM).

*Also at Gruppo Nazionale di Struttura della Materia del Consiglio Nazionale delle Ricerche, I-98100 Messina, Italy.
[1]D. W. Fisher, Phys. Rev. B **8**, 3576 (1973).
[2]B. Sonntag and F. C. Brown, Phys. Rev. B **10**, 2300 (1974).
[3]B. M. Davies and F. C. Brown, Phys. Rev. B **25**, 2997 (1982).
[4]Y. Ohno, K. Hirama, S. Nakai, S. Sugiura, and S. Okada, Phys. Rev. B **27**, 3811 (1983).
[5]C. Webb and P. M. Williams, Phys. Rev. B **11**, 2082 (1975).
[6]H. W. Myron and A. J. Freeman, Phys. Rev. B **9**, 481 (1974).
[7]A. Zunger and A. J. Freeman, Phys. Rev. B **16**, 906 (1977).
[8]C. Umrigar, D. E. Ellis, Ding-Sheng Wang, H. Krakauer, and M. Posternak, Phys. Rev. B **26**, 4935 (1982).
[9]P. Krusius, J. von Boehm, and H. Isomaki, J. Phys. C **8**, 3788 (1975).
[10]G. A. Benesh, A. M. Woolley, and C. Umrigar, J. Phys. C **18**, 1595 (1985).
[11]J. E. Hahn, R. A. Scott, K. O. Hodgson, S. Doniach, S. R. Dejardins, and E. I. Salomon, Chem. Phys. Lett. **88**, 595 (1982).
[12]A. Šimůnek, G. Dräger, W. Czolbe, O. Brümmer, and F. Lévy, J. Phys. C **18**, 1605 (1985).
[13]PULS Activity Report LNF 80/79, 1980 (unpublished); PULS Activity Report LNF 82/51, 1982 (unpublished).
[14]F. Antonangeli, M. L. Apicella, A. Balzarotti, L. Incoccia, and M. Piacentini, Physica **105B**, 25 (1981).
[15]J. A. Bearden and A. F. Burr, Rev. Mod. Phys. **39**, 125 (1967).
[16]*Electronic Structure and Electronic Transitions in Layered Materials: Recent Developments,* Vol. 7 of *Physics and Chemistry of Materials with Low-Dimensional Structures, Series A: Layered Structures,* edited by V. Grasso (Reidel, Dordrecht, in press).
[17]P. Lloyd and P. V. Smith, Adv. Phys. **21**, 69 (1972).
[18]B. L. Gyorffy and G. M. Stokes, in *Electrons in Finite and Infinite Structures,* edited by P. Phariseau (Plenum, New York, 1977).
[19]E. Condon and G. Shortley, *The Theory of Atomic Spectra* (Cambridge University Press, Cambridge, England, 1967).